

# Calcium-Sensitive Downregulation of the Transduction Chain in Rod Photoreceptors of the Rat Retina

Andreas Knopp and Hartmann Rüppel

Max-Volmer-Institut of Biophysical Chemistry, Technical University Berlin, Berlin, Germany

**ABSTRACT** In vertebrate rod outer segments phototransduction is suggested to be modulated by intracellular Ca. We aimed at verifying this hypothesis by recording saturated photosignals in the rat retina after single and double flashes of light and determining the time  $t_c$  to the beginning of the signal recovery. The time course of  $Ca_i$  after a flash was calculated from a change of the spatial  $Ca^{2+}$  concentration profile recorded in the space between the rods. After single flashes  $t_c$  increased linearly with the logarithm of flash intensity, confirming the assumption that  $t_c$  is determined by deactivation of a single species  $X^*$  in the phototransduction cascade. The photoresponse was shortened up to 45% if the test flash was preceded by a conditioning preflash. The shortening depended on the reduction of  $Ca_i$  induced by the preflash. The data suggest that the phototransduction gain determining the amount of activated  $X^*$  is regulated by a  $Ca_i$ -dependent mechanism in a short time period ( $<800$  ms) after the test flash. Lowering of  $Ca_i$  by a preflash reduced the gain up to 20% compared to its value in a dark-adapted rod. The relation between phototransduction gain and  $Ca_i$  revealed a  $K_{1/2}$  value close to the dark level of  $Ca_i$ .

## INTRODUCTION

In vertebrate rod outer segments (ROS), light activates a cascade of enzymatic reactions leading to a reduction of ion current flowing across the outer membrane (1–3). In a first step, light-activated rhodopsin  $Rho^*$  initiates a guanosine diphosphate (GDP)/guanosine triphosphate (GTP) exchange in the G-protein transducin and a liberation of the  $\alpha$ -subunit  $T_\alpha GTP$ . Binding of  $T_\alpha GTP$  to cyclic guanosine monophosphate (cGMP)-specific phosphodiesterase (PDE) abolishes the inhibitory function of the two PDE $_\gamma$  subunits, resulting in accelerated cGMP hydrolysis. Finally, lowering the cGMP concentration causes a closure of cGMP-dependent channels. Activation of one rhodopsin interrupts the inflow of  $>10^5$   $Na^+$  and  $Ca^{2+}$  ions into the cell. By reducing the  $Ca^{2+}$  influx through the cGMP-dependent channels (4–6), illumination reduces the  $Ca^{2+}$  concentration  $Ca_i$  in the ROS (7–14). Reduction of  $Ca_i$  is suggested to play a prominent role in regulating sensitivity and light adaptation: A desensitization of the rod during exposure to steady light and an accelerated recovery of the light-regulated conductance after flashes of light are both mediated by light-induced lowering of the  $Ca_i$  (15–17).

The reduction of  $Ca_i$  activates cGMP synthesis by guanylyl cyclase (18), which is thought to play a major role in light adaptation during background light (19). After saturating flashes, the reopening of the light-dependent channels is dramatically accelerated if guanylyl cyclase is allowed to be stimulated by a reduction of  $Ca_i$  (20). In addition to affecting guanylyl cyclase, a reduction of  $Ca_i$  was

suggested to 1), reduce the amplification within the transduction cascade (21–23); 2), reduce the lifetime of activated PDE (24); or 3), increase the affinity of cGMP-gated ion channels to cGMP (25). Each of these effects would represent a negative feedback mechanism attenuating the process of phototransduction.

After a saturating flash, the light-dependent channels are kept close despite guanylyl cyclase being rapidly activated by a fall of  $Ca_i$ . For reopening the channels, PDE needs to be deactivated to a distinct level at which cGMP production and cGMP hydrolysis are balanced again. Deactivation of PDE requires a preceding inactivation of  $Rho^*$  and  $T_\alpha GTP$ . Indeed, the time between flash and channel reopening is proportional to the logarithm of the saturating-flash intensity (26,27). This finding strongly suggests that the time of channel reopening is determined by the deactivation of only a single component  $X^*$  of the phototransduction chain, which is activated proportional to the flash intensity and deactivated by first-order kinetics. Recent experiments suggest that this species is  $T_\alpha GTP$  (23,28–30). A reduction of the number of  $X^*$  activated per  $Rho^*$  is suggested to contribute to light adaptation during steady background illumination and to desensitization after preflashes (22,31).

Herein, we studied an effect of  $Ca_i$  on the sensitivity of the phototransduction chain. Preflashes were applied to reduce  $Ca_i$  to a variable degree and the desensitization was tested by subsequent test flashes. For determination of  $Ca_i$ , we used our method of calculating  $Ca_i$  from the spatial profile of the extracellular  $Ca^{2+}$  concentration, which was determined by use of microelectrodes inserted into the photoreceptor layer of the isolated retina (8). Calcium-sensitive fluorescence probes used in amphibian rods are not applicable for recordings of preflash-induced  $Ca_i$  in rats because mammalian rods are much smaller and fluorescence itself affects the phototransduction.

Submitted January 31, 2006, and accepted for publication April 18, 2006.

Address reprint requests to Dr. A. Knopp, AG Behr, Institute for Neurophysiology, Charité-Universitätsmedizin Berlin, Tucholskystr. 2, D-10117 Berlin, Germany. Tel.: 49-30-450 528209; Fax: 49-30-450 539941; E-mail: andreas.knopp@charite.de.

© 2006 by the Biophysical Society

0006-3495/06/08/1078/12 \$2.00

doi: 10.1529/biophysj.106.082271

In our recordings, the cGMP channels reopened earlier when a preflash was given before the test flash. Our results strongly suggest that the phototransduction gain is reduced upstream to  $X^*$  as a consequence of a lowered  $\text{Ca}_i$  induced by the preflash.

## MATERIAL AND METHODS

### Materials

Albino rats "Wistar" were purchased from Schering AG (Berlin, Germany). Ca-Ionophore Cocktail A, carbontetrachloride ( $\text{CCl}_4$ ), and trimethylchlorosilane ( $\text{Me}_3\text{SiCl}$ ) were obtained from Fluka (Neu Ulm, Germany). The  $\text{Ca}^{2+}$  ionophore A23187 was obtained from Sigma Chemie (Deisenhofen, Germany).

### Retinal preparation

Albino rats were kept in complete darkness for 2 h or more before they were sacrificed by peritoneal injection of 2 ml of the  $\text{Na}^+$  pentobarbiturat Nembutal (Ceva, Bad Segeberg, Germany). After cardiac arrest the eyes were enucleated and the bulbus was meridially cut and transferred into Ringer solution. After  $\sim 10$  min the retina was gently removed from the pigment epithelium and stored in Ringer solution at room temperature in darkness. For recordings, a piece of retina ( $\sim 1 \text{ mm}^2$ ) was placed receptor side up on a cellulose acetate filter (SM 11104 Satorius, Göttingen, Germany) and taken into the recording chamber. The preparation was carried out under dim red light.

### Solutions

Ringer solution was prepared after Hagins et al. (32), consisting of (in mM) 130 NaCl, 2.2 KCl, 0.18  $\text{Mg} \cdot 6 \text{ H}_2\text{O}$ , 11 Glucose, 1.3  $\text{KH}_2\text{PO}_4$ , 5.4  $\text{Na}_2\text{HPO}_4$ , 10 HEPES, pH 7.4 (NaOH). If not indicated otherwise, 0.25 mM  $\text{CaCl}_2$  was added to the Ringer solution.  $\text{Ca}^{2+}$  concentrations  $< 10 \mu\text{M}$  were adjusted by 10 mM EGTA.

### Recording chamber and photostimulation

The recording chamber consisted of a glass cuvette perfused with Ringer solution. The cuvette was thermostated by a Peltier element. From above the recording chamber a recording microelectrode was moved vertically between the photoreceptor cells by a stepper motor (AM2 M2, Bachofer, Reutlingen, Germany) with a step precision of  $\pm 0.1 \mu\text{m}$ .

The piece of retina in the recording chamber was illuminated by a wave guide from below the recording chamber. Light flashes were produced by an LED which could be pulsed for generation of short flashes. Light intensity was attenuated by neutral density filters (Kodak No. 96, Eastman Kodak Co., Rochester, NY). We denoted the flash intensity  $I_f$  as the number of photoisomerizations  $\text{Rho}^*$  produced in an ROS per flash. The scaling is based on the finding that in a dark-adapted retina, flash activation of 30  $\text{Rho}^*/\text{ROS}$  produces 50% reduction of the dark current (33).

### Electrophysiology

Microelectrodes were pulled from borosilicate glass tubing. Single-barrel microelectrodes were used if only the field potential was recorded. They consisted of a resistance of 4–8 M $\Omega$  after filling with Ringer solution. The field potential was considered to be proportional to the circulating photoreceptor current (8). Light flashes reduce the field potential (photosignal) concomitantly to the receptor current. Photosignal amplitudes reached a maximum of 30–150  $\mu\text{V}$  as measured after bright saturating flashes. Double-

barreled microelectrodes (tip diameter 1.5–3.0  $\mu\text{m}$ ) were used for simultaneous recordings of field potential and extracellular  $\text{Ca}^{2+}$  concentration. The barrel designated for voltage measurement was filled with Ringer solution. The second barrel was prepared as a  $\text{Ca}^{2+}$ -selective microelectrode. It was filled with a solution of 10 mM  $\text{CaCl}_2$  and 135 mM KCl and silanized by repetitive suction of  $\text{Me}_3\text{SiCl}/\text{CCl}_4$  solution (5 vol %) into the tip. Finally, the silanized tip was equipped with a Ca-selective membrane by filling with an organic matrix containing 10% of the Ca ionophore ETH 1001 (Ca-Ionophore Cocktail A). The  $\text{Ca}^{2+}$ -selective barrels of microelectrodes selected for measurements had a resistance of 5–10 G $\Omega$ , a risetime of 50–80 ms, and a steepness of 27–30 mV per decade determined with test solutions containing 0.1–1 mM  $\text{CaCl}_2$  and 150 mM NaCl. A reference electrode of 4–8 M $\Omega$  filled with Ringer solution was situated  $\sim 100 \mu\text{m}$  above the retina. Changes of field potential (photosignal) and extracellular  $\text{Ca}^{2+}$  concentration (Ca signals) were recorded with a voltage difference amplifier of high-input impedance (Neuro Hel IRIS, Meyer, München, Germany) and further amplified and RC lowpass-filtered with a cascade of difference amplifiers. The overall transmission band was 13 Hz. The amplifier assembly enabled a simultaneous recording of  $\text{Ca}^{2+}$  concentration and field potential.

### Determination of the net $\text{Ca}^{2+}$ flux and calculation of $\text{Ca}_i$

The time course of the free intracellular  $\text{Ca}^{2+}$  concentration  $\text{Ca}_i$  in the ROS after a preflash was determined as described previously (8,34). A double-barreled electrode was moved into the photoreceptor layer by steps of  $\Delta z = 8 \mu\text{m}$ . At each step position three flash stimuli were applied. Photo- and Ca signals were recorded and averaged. Ca signals were obtained at any step position, whereas photosignals were obtained only after the electrode tip had passed the photoreceptor tips at  $z = 0$  (Fig. 1, A and B). The series of Ca signals obtained by this procedure represent the flash-induced change of the extracellular  $\text{Ca}^{2+}$  concentration as a function of penetration depth  $z$  and time  $t$  ( $c = c(z, t)$ ). Ca signals were smoothed three times alternately in time and penetration depth (bandwidth after smoothing 0.4 Hz). By considering that  $\text{Ca}^{2+}$  ions diffuse in the extracellular space only along gradients parallel to the  $z$  axis of the rods (8–10), the one-dimensional diffusion equation

$$q(z, t) = \frac{\partial c}{\partial t} - D \times \left( \frac{\partial^2 c}{\partial z^2} + \frac{1}{F} \times \frac{dF}{dz} \times \frac{\partial c}{\partial z} \right) \quad (1)$$

was used to calculate the source function  $q(z, t)$ , which describes at a position  $z$  the  $\text{Ca}^{2+}$  flux across the rod outer membrane.  $F = F(z)$  is the cross-section area of the space between the rods, which was estimated by assuming that the electrode tip is surrounded by four ROS that at  $z = 0$  have a radius of 0.9  $\mu\text{m}$  (32). At  $z > 0$ ,  $F(z)$  was derived from the longitudinal resistance in the extracellular space per unit length (32), which is inversely proportional to  $F(z)$ .

The value of  $q$  determines whether a change of the  $\text{Ca}^{2+}$  concentration at a position  $z$  is due to diffusion ( $q = 0$ ) or if sources ( $q > 0$ ) or sinks ( $q < 0$ ) in the rod outer membrane do contribute. From  $q(z, t)$  the time course of the  $\text{Ca}^{2+}$  efflux  $\Delta Q_z$  after a flash of light was determined at different positions along a photoreceptor cell (Fig. 1 C). The net  $\text{Ca}^{2+}$  flux  $J_{\text{OS}}$  from the whole ROS was calculated by integration of  $q$  over the length of an ROS, i.e., from  $z = 0$  to  $z = 25 \mu\text{m}$

$$J_{\text{OS}}(t) = \int_0^{25\mu} q(z, t) \times N_A^{-1} \times F(z) dz, \quad (2)$$

where  $N_A$  is Avogadro's constant (Fig. 1 D). From  $J_{\text{OS}}(t)$ ,  $\text{Ca}_i(t)$  was calculated by using a model of Miller and Korenbrot (35). In this model  $J_{\text{OS}}(t)$  represents the sum of the  $\text{Ca}^{2+}$  influx  $J_{\text{in}}$  through the light-dependent channels and the  $\text{Ca}^{2+}$  efflux  $J_{\text{eff}}$  caused by the  $\text{Na}^+/\text{K}^+ - \text{Ca}^{2+}$  exchanger (35–37):

$$J_{\text{OS}}(t) = J_{\text{eff}}(t) + J_{\text{in}}(t). \quad (3)$$

In the dark, the Ca influx  $J_{\text{d,in}}$  and the efflux  $J_{\text{d,eff}}$  are balanced and  $J_{\text{OS}}$  is zero.  $J_{\text{in}}$  is assumed to be a constant fraction of the light-sensitive current.

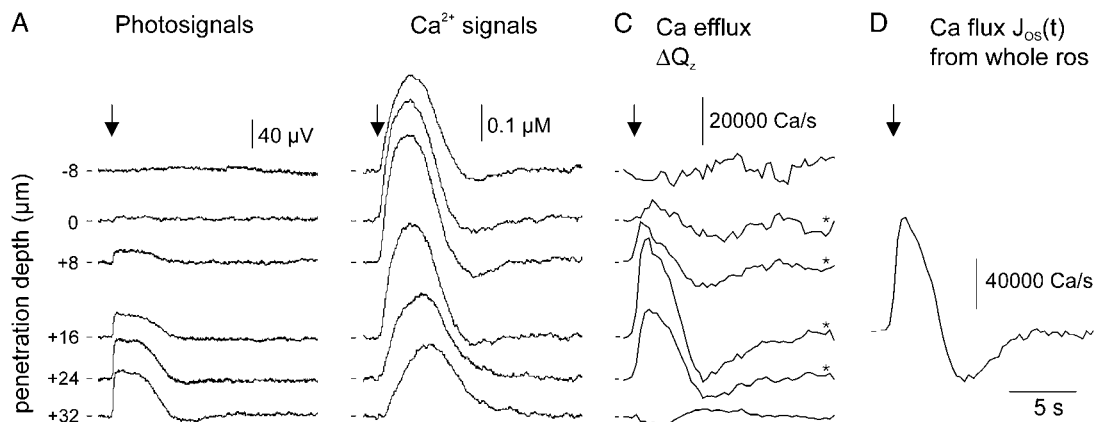


FIGURE 1 Determination of Ca flux  $J_{OS}$  from the outer segment. Temperature 30°C;  $Ca^{2+}$  concentration in the Ringer solution 0.1 mM. (A) Photosignals in response to a saturating flash of light (indicated by arrow). Recordings were done by positioning the tip of a double-barreled electrode in different depths  $z$  above ( $< 0 \mu m$ ) and within ( $> 0 \mu m$ ) the photoreceptor layer. At  $0 \mu m$  the electrode tip passed the tips of the outer segments. Each trace is an average of three single recordings. (B) Ca signals recorded at different positions  $z$  simultaneously with the photosignals. (C) Ca efflux: extrusion of  $Ca^{2+}$  ions  $\Delta Q_z(t) = q(z,t) \times N_A \times F \times \Delta z$  from an ROS into the volume  $V_z = F \times \Delta z$  at the position  $z$  of the recording electrode ( $F$  is the cross-section area between rods and  $\Delta z$  is the step width of the electrode). The source function  $q(z,t)$  was calculated from Ca signals in B by use of Eq. 1. (D)  $Ca^{2+}$  flux  $J_{OS}$  from the outer segment obtained by integration of  $q$  from  $z = 0-24 \mu m$  (Eq. 2).

Hence, when  $A(t)$  is the amplitude and  $A_{max}$  is the maximum amplitude of the photosignal, it follows that

$$J_{eff}(t) = J_{OS}(t) - J_{d,in} \times \frac{A_{max} - A(t)}{A_{max}}. \quad (4)$$

After a saturating photoresponse  $J_{in}(t)$  is abruptly blocked and  $J_{OS}(t)$  raises to a maximum value  $J_{OS,max}$  (Figs. 1 D and 2 C) that represents the  $Ca^{2+}$  efflux when  $Ca_i$  is close to its dark level  $Ca_d$ . By taking into account that after the flash a maximum hyperpolarization of  $-25$  mV activates the  $Na^+/K^+-Ca^{2+}$  exchanger by 37% (35,38,39), it follows that  $J_{d,in} = J_{d,eff} = J_{OS,max}/1.37$ . Finally,  $Ca_i/Ca_d$  was calculated supposing that  $J_{eff}$  is proportional to  $Ca_i$ . As an approximation, we assumed that hyperpolarization follows the time course of the photosignal (35,40). Then, it is

$$Ca_i/Ca_d = J_{eff}(t)/J_{d,eff} \times \frac{1}{1 + 0.37 \times A(t)/A_{max}}. \quad (5)$$

Recordings of the spatial  $Ca^{2+}$  concentration were time consuming. Therefore, if not stated otherwise, the experiments were carried out at 23°C instead of at physiological temperature to improve the long-term stability of the retinal tissue.

## RESULTS

### Deactivation time $\tau_X$ determined from photosignals evoked by single flashes

Photosignals were recorded in response to flashes of increasing light intensity (Fig. 2 A). From signals reaching maximum amplitude, the signal length  $t_c$  was determined. We defined  $t_c$  as the time between the flash given in the dark-adapted state and the return of the photosignal to the half-maximum amplitude (see Fig. 2 B, upper trace). Between 60 and 3000 Rho\*/ROS induced per flash,  $t_c$  increases linearly with  $\log(I_f)$  (Fig. 2 C, upper trace). The slope  $\tau_X$  was considered to represent the lifetime of one species  $X^*$  of the

transduction cascade (Appendix 1). The average value of  $\tau_X$  was  $1.8 \pm 0.5$  s ( $n = 5$ ) at 23°C, agreeing well with  $\tau_X = 1.7-2.4$  s obtained from tiger salamander and toad rods (20,27,28,31). Like in rods of tiger salamander,  $t_c$  deviated from linearity at bright flashes: at  $I_f > 3000$  Rho\*/ROS,  $t_c$  was longer than expected from linear extrapolation (Fig. 2 C, upper trace).

Photoresponses that were just saturating showed an exponential recovery exhibiting a time constant  $\tau_{rec}$  equal to  $\tau_X$  (Fig. 2, C and D). At increasing flash intensity the recovery of the photosignals was slowed down (Fig. 2 A). Accordingly,  $\tau_{rec}$  increased (Fig. 2 C, lower trace). Here, a difference between  $\tau_X$  and  $\tau_{rec}$  was apparent: At highest flash intensity,  $\tau_{rec}$  increased sixfold, whereas  $\tau_X$  increased only by a factor of 2.5. Occasionally,  $\tau_{rec}$  began to increase at flash intensities slightly above saturation level, whereas higher flash intensities were necessary to cause a deviation of  $t_c$  from linearity (see, e.g., Fig. 6 B). Therefore, we suggest that  $\tau_{rec}$  and  $\tau_X$  may be affected by different mechanisms. Herein, we focused upon  $\tau_X$ , because it is assumed to represent the lifetime of  $X^*$  (see Discussion).

### Flash responses are shortened after a preceding conditioning flash

In amphibian rods a test flash produces a shorter photoresponse if it is preceded by a preflash (6,31). We obtained similar results in rat rods (34). In double-flash experiments, we illuminated the retina by a saturating conditioning preflash before applying the test flash. Representative photosignals in response to a saturating test flash with and without a preflash are shown in Fig. 2 B. The signal length  $t'_c$  was defined as the length of the test-flash-induced photosignal produced after a

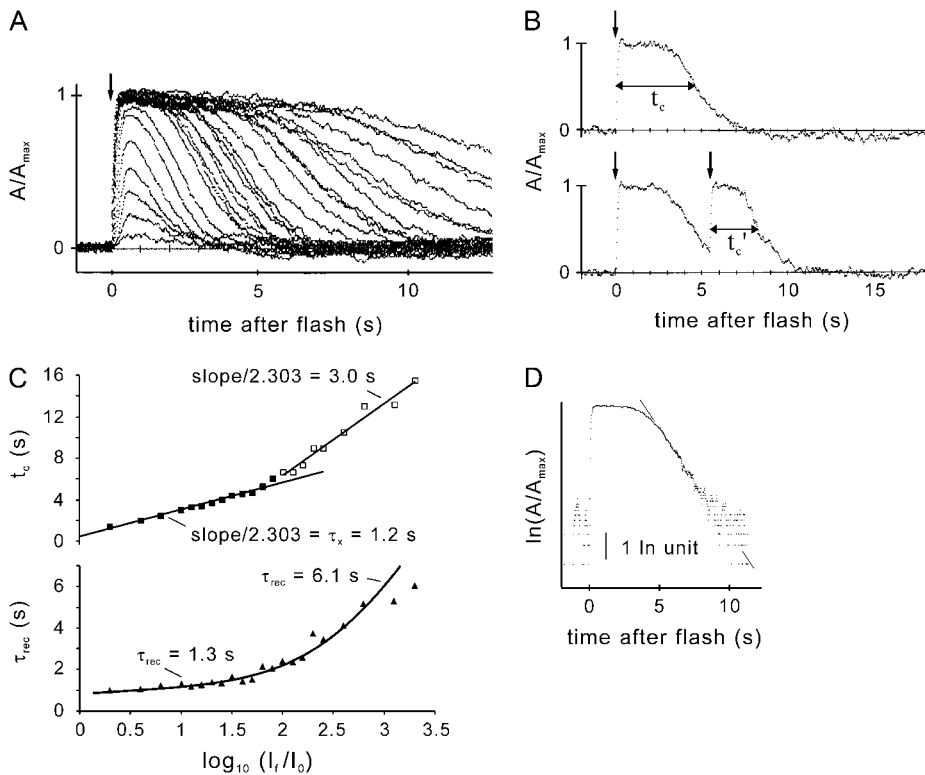


FIGURE 2 Photosignals in response to flashes of light (indicated by arrows) given to dark- or flash-adapted retina. Traces are averages of two to three single responses. (A) Dark-adapted retina was exposed to flashes of light that excited 3.8, 7.5, 15, 30, 60, 120, 190, 300, 380, 475, 600, 750, 950, 1200, 1500, 1900, 2400, 3000, 3800, 4750, 6000, 7500, 12,000, 19,000, 38,000, and 60,000 Rho\*/ROS. (B) Different retina from that shown in A. (Upper trace) A saturating single test flash was applied to a dark-adapted retina. The signal length  $t_c$  is determined as time between the flash and the recovery of the photosignal to 50% of the maximum amplitude. The signal recovers with a time constant  $\tau_{\text{rec}} = 1.4$  s. (Lower trace) Two flashes of the same intensity as used in the upper trace, separated by 5.4 s. The first conditioning flash produces a photosignal of identical time course to that indicated in the upper trace. The test flash produces a photosignal with reduced length  $t'_c$  and steeper falling phase ( $\tau'_{\text{rec}} = 0.9$  s). In this trace,  $t'_c$  is reduced to  $\sim 50\%$  compared with  $t_c$ . (C, upper trace) Signal lengths  $t_c$  obtained after single flashes as a function of the logarithm of the flash intensity. The arbitrary unit  $I_0$  was taken as 30 Rho\*/ROS. The relation  $t_c = \tau_X \times \ln(I_f/I_0)$  is valid over a range of 60–3000 Rho\*/ROS. From the slope,  $\tau_X$  was determined to be 1.2 s in this experiment. At higher intensities the slope increases to 3.0 s. (Lower trace)  $\tau_{\text{rec}}$  plotted versus  $\log(I_f/I_0)$ .  $\tau_{\text{rec}}$  increases from 1.3 s to 6.1 s. (D) Logarithmic plot of a photosignal. The recovery phase of the signal is exponential. Time constant  $\tau_{\text{rec}} = 1.3$  s.

preflash (Fig. 2 B, lower trace). After the preflash, the test flash produces a remarkably shortened photosignal:  $t'_c$  is only half as long as  $t_c$  which is the signal length obtained without a preflash.

In a first series of experiments, we applied a test flash at variable times  $\Delta t_f$  after the preflash. The dependence of  $t'_c/t_c$  on  $\Delta t_f$  is shown in Fig. 3 A and the time course of the preflash-induced photoresponse  $A(t)/A_{\max}$  is shown in Fig. 3 B. The quantity  $1 - A(t)/A_{\max}$  represents the receptor current flowing at the moment when the test flash was given. At  $\Delta t_f = 0$ , it was  $t'_c/t_c > 1$  because test and preflash coincide. This is equivalent to exposing the dark-adapted retina by a flash consisting of the sum of pre- and test-flash intensity. The effect is predicted by Eqs. A3 and A5 (Appendixes 1 and 2, respectively) if the intensity of the preflash is of similar order to or larger than the test-flash intensity. When the test flash was applied during the period of completely interrupted dark current,  $t'_c/t_c$  was reduced with increasing  $\Delta t_f$  to a minimum of  $t'_c/t_c = 0.6$ . Fitting to a monoexponential decay yielded a decay with a constant  $\Delta t_c = 4.4$  s to a minimum limit value  $t'_c/t_c = 0.46$ . The minimum of  $t'_c/t_c$  appeared when the test flash was given during the process of reopening of light-dependent channels. Further increase of  $\Delta t_f$  leads to a recovery of  $t'_c/t_c$  before having reached the minimum limit value. At  $14 \pm 1$  s after the preflash, the receptor current recovered to 95% of the dark level. However, a test flash

given at that time still produced a photosignal with a reduced signal length  $t'_c$ . Recovery to 95% of  $t'_c/t_c$  was observed when the test flash was applied at  $\Delta t_f = 17 \pm 1$  s after the preflash. Hence, it was suggested that after a preflash, the recovery of  $t'_c$  shortening was delayed with respect to recovery of the light-dependent conductance. Average values for  $\Delta t_c$  and the minimum limit value of  $t'_c/t_c$  were  $2.3 \pm 0.7$  s and  $0.44 \pm 0.14$  ( $n = 11$ ), respectively.

The decrease of  $t'_c/t_c$  to values  $< 1$  is in contrast to the concept that the intermediate  $X^*$  of the transduction chain that dominates the duration of phototransduction is activated with a constant gain. Calculation by use of this concept (Eq. A5, Appendix 2) yielded that by increasing  $\Delta t_f$ ,  $t'_c/t_c$  should decay steadily from the maximum value at  $\Delta t_f = 0$  and converge against 1 (Fig. 3 A, upper trace). For any value of  $\Delta t_f$ , it is  $t'_c/t_c \geq 1$ . This discrepancy between calculation and measured data demands a modification of this concept (see Discussion).

### Shortening of $t'_c$ depends on a reduction of the $\text{Ca}^{2+}$ concentration in the ROS

It is feasible that the effect of the preflash on  $t'_c$  is mediated by  $\text{Ca}_i$ . To test this hypothesis we determined how the preflash reduced  $\text{Ca}_i$  before the test flash was applied (briefly described in Materials and Methods; see also Knopp and R  ppel (8)). In a first step, we determined the time course of the net  $\text{Ca}^{2+}$

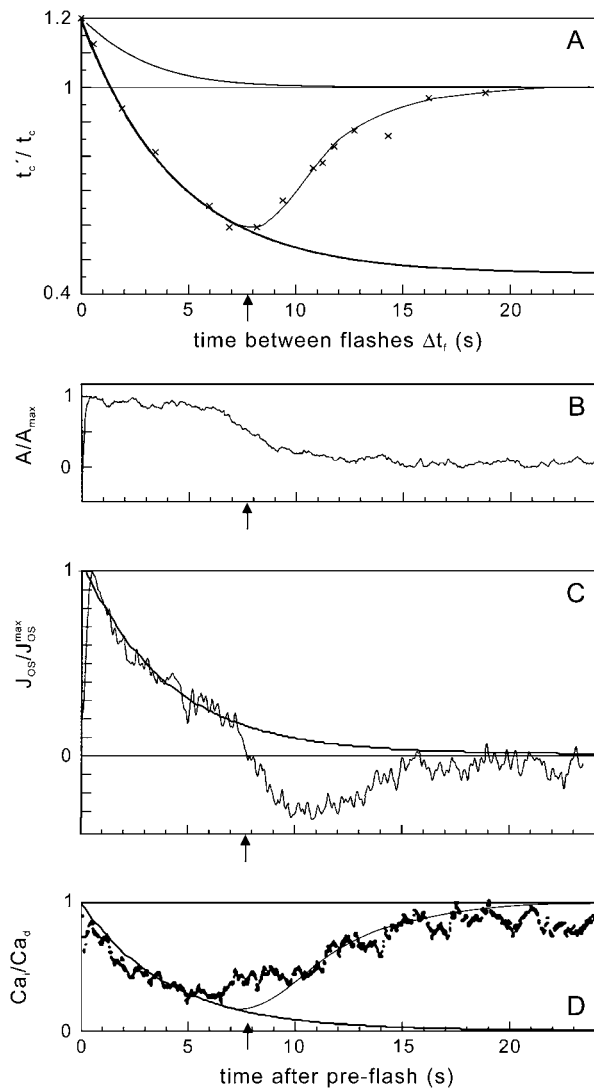


FIGURE 3 Shortening of  $t'_c$  induced by a preflash and correlation to  $Ca_i(\Delta t_f)$  present at the moment of the test flash. It was  $\tau_X = 2.3$  s, and  $t_c = 7.5$  s. Intensities of pre- and test flash were identical. (A)  $t'_c/t_c$  versus time  $\Delta t_f$  by which the test flash followed after the preflash. (Upper trace) Calculation according to Eq. A5. It is  $t'_c = 1.2 \times t_c$  at  $\Delta t_f = 0$ , i.e., when pre- and test flash coincide. Upon increasing  $\Delta t_f$ ,  $t'_c/t_c$  is steadily reduced approaching 1. (Lower trace) Recorded values of  $t'_c/t_c$  plotted against  $\Delta t_f$ . From the maximum value of 1.2 at  $\Delta t_f = 0$  s,  $t'_c/t_c$  is reduced to a minimum value 0.6 at  $\Delta t_f = 7.8$  s, which occurs when the test flash is applied during recovery of the dark current. At the same time,  $Ca_i$  has reached a minimum level (see arrows in A, B, and D). At  $\Delta t_f \geq 20$  s,  $t'_c$  has returned to the dark value  $t_c$ . Here and in the following figures the recovery of  $t'_c/t_c$  to the dark state has been fitted to data by eye (see solid line). The reduction of  $t'_c/t_c$  with growing  $\Delta t_f$  was fitted by an exponential decline with  $\tau_{tc} = 4.4$  s to a minimum limit value  $t'_c/t_c = 0.46$  (bold line). (B) Photosignal caused by a preflash alone. Plateau length  $\sim 6$  s. The photosignal represents the time course of  $Ca^{2+}$  influx  $J_{in}$  before applying the test flash (see Materials and Methods). (C)  $J_{OS}$  representing net  $Ca^{2+}$  flux in response to the preflash. From the maximum value ( $1 \times 10^5$   $Ca^{2+}$  s $^{-1}$ ),  $J_{OS}$  declines exponentially with a time constant of 4 s during completely interrupted dark current. (D) Time course of  $Ca_i$  in response to the preflash normalized to the dark concentration  $Ca_d$ .  $Ca_i$  is exponent-reduced with  $\tau_{Ca} = 4$  s. The  $Ca^{2+}$  concentration  $Ca_i(t)$  at a time  $t$  after the preflash is equivalent to the  $Ca^{2+}$  concentration  $Ca_i(\Delta t_f)$  present at the moment of the test flash applied at a time  $\Delta t_f$  after the preflash:  $Ca_i(t) = Ca_i(\Delta t_f)$ .

efflux from the ROS,  $J_{OS}(t)$ , during the preflash-induced photosignal (Fig. 3 B). When the  $Ca^{2+}$  influx  $J_{in}$  through light-dependent channels was abruptly blocked (Fig. 3 B)  $J_{OS}(t)$  steeply increased to a maximum followed by an exponential decay with a time constant of 4 s (Fig. 3 C). This exponential decay lasted as long as the plateau phase of the photosignal. When the photoreceptor current recovered to  $\sim 50\%$ ,  $J_{OS}(t)$  reversed to negative values, indicating that  $Ca^{2+}$  flowed back into the  $Ca^{2+}$ -depleted ROS;  $\sim 20$  s after the preflash,  $J_{OS}(t)$  was zero again, indicating that  $J_{eff}$ ,  $J_{in}$ , and  $Ca_i$  recovered to the dark value.

During the whole plateau phase of a photosignal  $J_{in}$  is completely blocked so that during this time interval  $J_{OS}(t)$  exclusively represents  $J_{eff}$ , which during the plateau phase is proportional to  $Ca_i$ . Necessarily,  $Ca_i$  must decay with the same time constant as  $J_{OS}(t)$ . The time course of  $Ca_i$  is shown in Fig. 3 D. It shows an exponential decay during the plateau phase of the preflash-induced photosignal. The time constant was  $\tau_{Ca} = 4$  s. Similar results are obtained in five out of five experiments, showing a strong correlation between  $t'_c(\Delta t_f)$  and  $Ca_i(\Delta t_f)$ : 1),  $Ca_i(\Delta t_f)$  and  $t'_c(\Delta t_f)$  decrease exponentially with equal time constants  $\tau_{Ca} = \tau_{tc}$ ; 2), the minimum of  $t'_c/t_c$  coincides with the minimum of  $Ca_i$  ( $\Delta t_f$ ); and 3), the shortening of  $t'_c/t_c$  is abolished as soon as the test flash is applied after  $Ca_i$  has recovered to the dark level.

We next examined whether the shortening of  $t'_c$  is affected when the reduction of  $Ca_i$  is prevented. We fixed  $Ca_i$  to the  $Ca^{2+}$  concentration of the external medium by adding 20  $\mu M$  of the  $Ca^{2+}$  ionophore A23187 to the Ringer solution. The result of a typical experiment is shown in Fig. 4. The presence of A23187 prevented a preflash-induced shortening of  $t'_c$  below the value of  $t_c$ . Instead, the dependence of  $t'_c$  on  $\Delta t_f$  now obeyed Eq. 5A (Fig. 4, upper curve). The same result was obtained with three other retinæ, giving strong

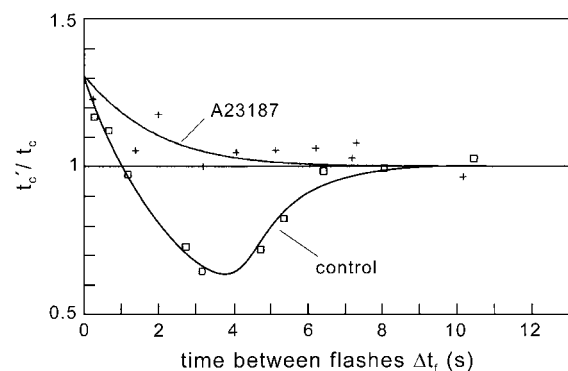


FIGURE 4 Proof that the shortening of  $t'_c$  is due to the fall of  $Ca_i$  induced by the preflash. Test and preflash had the same intensity. (Lower trace) Control recording, with  $t_c = 3.8$  s and  $\tau_X$  determined to be 1.7 s. (Upper trace) Twenty micromoles of A23187 was applied to shortcut  $Na^+/K^+$ - $Ca^{2+}$  exchanger. Ringer solution contained 100 nM  $Ca^{2+}$ . The extensive reduction of  $t'_c/t_c$  is abolished. The solid line represents a data fit of Eq. A5, using the experimental parameters  $R_{0,pre}/R_0 = 1$  and  $t_c = 3.4$  s. The fit yielded  $\tau_X = 1.51$  s.

evidence that the shortening of  $t'_c$  below the value of  $t_c$  (Fig. 4, lower curve) is caused by a reduction of  $\text{Ca}_i$ .

We also tested whether the congruence of  $\tau_{\text{Ca}}$  and  $\tau_{\text{tc}}$  is preserved if the temperature is changed (Fig. 5). After raising the temperature from 23 to 30°C, the preflash produced a photosignal with an accelerated recovery and a shortened plateau phase (lower traces). Similar effects of temperature have already been studied in rat and amphibian rods (41–43). In correspondence to the faster reopening of the light-regulated channels at 30°C,  $J_{\text{OS}}$  indicated an earlier reentry of  $\text{Ca}^{2+}$  ions (middle traces). Moreover,  $J_{\text{OS}}$  decayed faster, suggesting an accelerated depletion of  $\text{Ca}_i$  after the preflash. Concomitantly, in double-flash experiments the reduction of the signal length  $t'_c$  was accelerated (upper traces). During the plateau phase of the photosignal,  $J_{\text{OS}}$  decays with a time constant equal to  $\tau_{\text{Ca}}$  (see above). Determination of the time constants yielded that the rise of temperature reduced  $\tau_{\text{Ca}}$  from 3.4 to 0.7 s and  $\tau_{\text{tc}}$  from 3.1 to 0.9 s. A similar result was obtained in one additional experiment. Hence, within an error limit of 10%, independent of the temperature, it was  $\tau_{\text{Ca}} = \tau_{\text{tc}}$ , i.e.,  $t'_c$  was reduced proportional to the  $\text{Ca}_i$  present in the moment of the test flash. Averaging the differences,  $\tau_{\text{Ca}} - \tau_{\text{tc}}$ , obtained in all experiments at 23° and 30°C yields  $0.04 \pm 0.30$  s ( $n=5$ ).

### Variation of the preflash intensity

In our next approach, we tested whether the preflash-induced shortening of  $t'_c$  depends on the intensity of the preflash. We

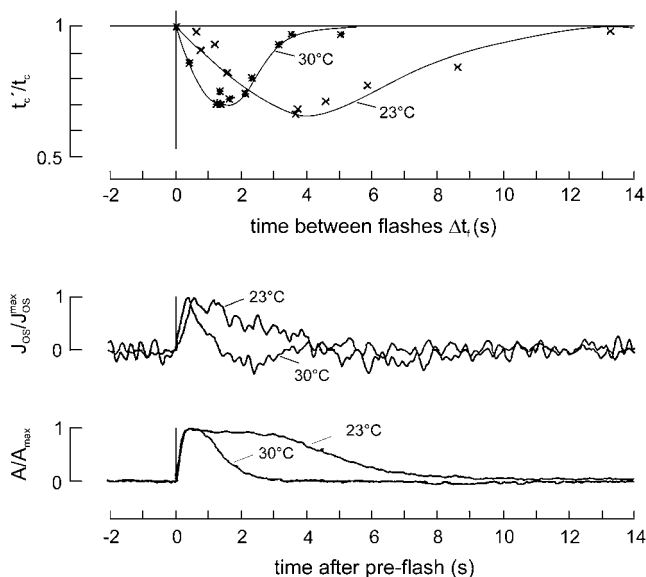


FIGURE 5 Effect of temperature on the shortening of  $t'_c$ . Recordings were conducted at one piece of retina at 30° and 23°C. Preflash excited 600 and test flash 3000 Rho\*/ROS. (Upper)  $t'_c/t_c$  plotted versus time  $\Delta t_f$  by which the test flash followed after the preflash. Note that at  $\Delta t_f = 0$ , it is  $t'_c \approx t_c$ . (Middle) Time course of normalized net  $\text{Ca}^{2+}$  flux  $J_{\text{OS}}$  in response to the preflash. Maximum values are 6 and  $1 \times 10^5$   $\text{Ca}^{2+}$ /s at 23 and 30°C, respectively. (Lower) Normalized photosignals in response to the preflash.

created a data set of  $t'_c/t_c$  values (Fig. 6 A) by successively increasing the preflash intensity from 150 to 2400 Rho\*/ROS (traces a–d). The intensity of the test flash was kept constant at 2400 Rho\*/ROS. All traces a–d show an exponential reduction of  $t'_c/t_c$  with growing  $\Delta t_f$  independent of the preflash intensity with the same time constant  $\tau_{\text{tc}} = 2.9 \pm 0.1$  s. At each preflash intensity,  $t'_c/t_c$  showed a minimum when the test flash was applied during the recovery phase of the preflash-induced photosignal. The minimum was more pronounced the longer the preceding saturation lasted.

For traces a–c in Fig. 6 A, the extrapolated initial value of ( $t'_c/t_c$ ) at  $\Delta t_f = 0$  was  $\sim 1$  because the preflash intensity was less than the test flash intensity (Eq. A5). At increasing  $\Delta t_f$ ,  $t'_c$  was reduced independent of the intensity of the preflash (Fig. 6 A, bold trace). Trace d, however, showed a remarkable deviation from traces a–c. This deviation is explained by Eq. A3, which is valid for single-flash experiments (Appendix 1), and by Eq. A5, which was derived for double flashes without considering a desensitization (Appendix 2). According to Eqs. A5 and A3, at  $\Delta t_f = 0$ , when pre- and test flash coincide, it is  $t'_c/t_c \approx 1$  if the preflash is weaker than the test flash (traces a–c). In the case of the same intensity for pre- and test flash (trace d),  $t'_c/t_c$  was calculated to be 1.16. Hence, the calculation was in good agreement with the measured data at  $\Delta t_f = 0$ . The further deviation of trace d at  $\Delta t_f > 0$  was produced by residual  $X^*$  originating from the preflash, which was still active when the test flash was given. This residual  $X^*$  prolonged the  $t'_c/t_c$  of trace d with respect to traces a–c. With increasing time between pre- and test flash, the influence of residual  $X^*$  on  $t'_c$  lessened, and all traces converged exponentially against the same minimum value. Therefore, the deviation of trace d minimizes with  $\Delta t_f$ .

We also tested whether  $\tau_X$  is affected by a preflash. First, a series of single flashes was given to the dark-adapted retina. The plot of  $t_c$  against the  $\log(I_f)$  yielded  $\tau_X = 1.31 \pm 0.2$  s (Fig. 6 B, lower). The corresponding time constant  $\tau'_X$  in the flash-adapted retina was determined by giving a preflash of constant intensity before the test flash. The test flashes were given at 50% recovery of the preflash-induced photosignal, i.e., when  $t'_c$  and  $\text{Ca}_i$  were at a minimum (cf. Fig. 3). Plotting  $t'_c$  against  $\log(I_f)$  yielded  $\tau'_X = 1.52 \pm 0.3$  s and  $1.32 \pm 0.3$  s at a preflash intensity exciting 75.5 and 600 Rho\*/ROS, respectively (Fig. 6 B, lower). Thus, a preflash produced a parallel shift but did not change the slope of the semilogarithmic plot, indicating that the preflashes did not affect  $\tau_X$ . Rather, the shift in the semilogarithmic plot points to a preflash-induced reduction of the transduction gain  $\gamma$ . In Fig. 6 C the relative decrease of  $\gamma$  versus  $\Delta t_f$  has been determined from the data of the signal-length reduction (see Discussion for details).

If in this retina a single flash just reached saturation level, the photosignal recovered with  $\tau_{\text{rec}} = 1.1$  s (Fig. 6 B, upper and middle). Hence,  $\tau_{\text{rec}}$  was similar to  $\tau_X$  at this flash intensity. By further increasing the flash intensity,  $\tau_{\text{rec}}$  increased considerably. In contrast,  $\tau_X$  was constant over the whole range of tested flash intensities. Interestingly, preflashes

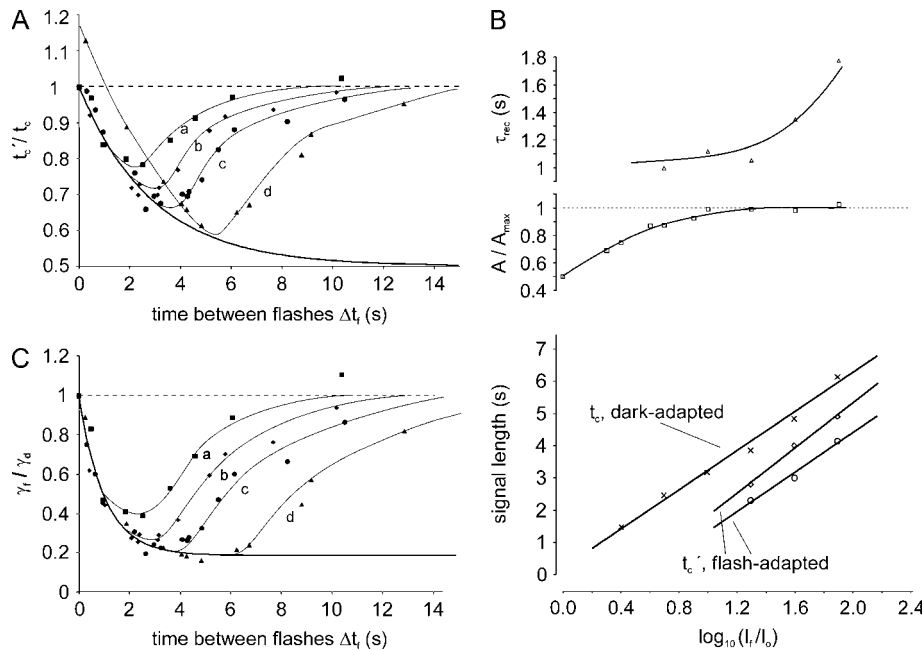


FIGURE 6 Double-flash recordings with variation of the preflash intensity. Preflash intensity  $I_{pre} = 150$  (a), 300 (b), 600 (c) and 2400 (d) Rho\*/ROS. The test-flash-activated  $I_f = 2400$  Rho\*/ROS throughout. The test flash produced a photosignal with  $t_c = 6.13$  s. (A)  $t'_c/t_c$  as a function of time  $\Delta t_f$  between pre- and test flash. For each of traces a–d,  $t'_c/t_c$  is reduced exponentially with  $\tau_{rec} = 2.9$  s to a minimum limit value of 0.5 by increasing  $\Delta t_f$  as long as the test flash was given during completely reduced dark current. If  $I_{pre} \ll I_f$  (as in traces a–c),  $t'_c/t_c$  starts near 1 and shares a common decrease with growing  $\Delta t_f$  (bold line). With growing values for  $I_{pre}$  an increased deviation from the common trace is observed (most obviously for trace d, with  $I_{pre} = I_f$ ). This deviation depends on the relation  $R_{0,pre}/R_0$  in Eq. A5. (B, upper and middle) Time constant of the photosignal recovery  $\tau_{rec}$  and normalized photosignal amplitude in dependence of  $\log(I_f)$ . Flashes were applied to the dark-adapted retina. (Lower) Signal lengths plotted against  $\log(I_f)$  ( $I_0 = 30$  Rho\*/ROS). The slope is independent of whether a preflash was given before the test flash. (C) Gain  $\gamma_t$  of the transduction chain after a preflash versus  $\Delta t_f$ . The gain is normalized to its dark value  $\gamma_d$ . The values of  $\gamma_t/\gamma_d$  were calculated using Eq. A7 from the measured values of  $t'_c/t_c$  shown in A.

reduced  $\tau_{rec}$  back to or even below the value of  $\tau_X$  (Fig. 2, B and C). Moreover, a photosignal with a long plateau phase of several seconds showed a slow recovery ( $\tau_{rec} \gg \tau_X$ ) if it was evoked by one strong single flash, whereas it was followed by a fast recovery ( $\tau_{rec} \approx \tau_X$ ) if it was evoked by successive application of two or more saturating flashes of weak intensity (not shown). Therefore, the increase of  $\tau_{rec}$  does not depend on the plateau length or the level of  $Ca_i$  at the time when the channels reopen. Rather, unlike  $\tau_X$ ,  $\tau_{rec}$  seems to be sensitive to the conditions at which the rod is illuminated. Illumination favors a slow recovery if the rod is dark-adapted or the light intensity of flashes or constant light is high. Moderate light intensity and light adaptation of a rod seem to favor a fast recovery of the photosignal.

## DISCUSSION

Isolated retinæ of the albino rat were exposed to saturating test flashes with or without preceding preflashes. Photosignals, as well as the  $Ca^{2+}$  signal, were concomitantly recorded in the extracellular space between the rods. From this data,  $Ca_i$  was determined. The length of the photosignal, which is the time interval between the test flash and the return to the half-maximum signal amplitude, is remarkably reduced if the test flash is preceded by a conditioning preflash. This preflash-induced signal shortening runs parallel to the reduction of  $Ca_i$  present at the moment of the test flash. The signal shortening is completely abolished if reduction of  $Ca_i$  induced by the preflash is prevented. The data suggest that a test flash applied at reduced  $Ca_i$  activates the transduction cascade with reduced gain. The gain is defined as the amount of an

intermediate  $X^*$  of the transduction chain activated per absorbed photon. The  $K_{1/2}$  value of the gain reduction by means of  $Ca_i$  is estimated to be either similar to or above the dark level of  $Ca_i$ .

## Photoresponses evoked by single flashes

If single saturating flashes are given to the dark-adapted retina, the length  $t_c$  of the photosignal rises linear with  $\log(I_f)$  over a range of flash intensities of at least 1 log unit (Figs. 2 C and 6 B; cf. Pepperberg et al. (27)). Moreover, the recovery of the photosignals is approximately monoexponential, exhibiting a time constant  $\tau_{rec}$ . At low saturating-flash intensities, within the linear range of the semilogarithmic plot, the slope  $\tau_X$  is largely similar to  $\tau_{rec}$ . Comparable results were reported for amphibian rods (20,27,31). These results can be explained based on the idea that the recovery of these photosignals is dominated by the deactivation of one component  $X^*$  of the transduction cascade, with a lifetime  $\tau_X$  (27; see Appendix 1).

At brighter flash intensities the slope of the relation between  $t_c$  and  $\log(I_f)$  rises (Fig. 2 C). It is not clear yet whether the slope obtained at these flash intensities still represents the lifetime  $\tau_X$ . In amphibian rods, this deviation has been attributed to an unknown component of the transduction cascade with slow deactivation kinetics (27,44). It may also be explained by multiple photoisomerizations per disc leading to a  $T_\alpha GTP$  concentration that exceeds that of  $PDE_\gamma$ . This could decrease the rate at which  $T_\alpha GTP$  deactivates (45). Compared to  $\tau_X$ ,  $\tau_{rec}$  is more sensitive to flash intensity (Figs. 2 C and 6 B). It seems to be affected by

additional processes. Especially reentering  $\text{Ca}^{2+}$  ions may affect the time course of recovery by having an influence on guanylyl cyclase activity, membrane conductance, and the Hill coefficient of cGMP binding to the light-dependent channels. A  $\text{Ca}^{2+}$ -dependent GTPase accelerating factor may also affect  $\tau_{\text{rec}}$  (30). Double-flash experiments were performed within the linear range of the  $t_c$  versus  $\log(I_f)$  relation. Within this range, the variability of  $\tau_{\text{rec}}$  was estimated to affect  $t_c$  by  $<10\%$ . It was therefore considered negligible.

It was shown earlier that  $\tau_X$  is not influenced by guanylyl cyclase (20,28), suggesting that guanylyl cyclase is maximally activated during the plateau phase of a photosignal due to rapidly declining  $\text{Ca}_i$ . We found that after a saturating flash  $\text{Ca}_i$  is reduced with a time constant  $\tau_{\text{Ca}} = 2.3$  s at  $23^\circ\text{C}$  (8). A typical saturated photosignal shows a signal length of  $t_c = 2.5$ – $10$  s. Hence, assuming a dark level of  $\text{Ca}_i = 300$  nM (7,35,46),  $\text{Ca}_i$  is reduced to 4–100 nM, which should indeed result in a maximal activation of guanylyl cyclase when the channels reopen ( $K_{1/2} = 200$  nM  $\text{Ca}_i$ ) (47).

### Ca<sub>i</sub>-dependent gain reduction in double-flash experiments

We found that a preflash reduces the signal length in rat rods (Fig. 2 B; see also Knopp (34)). Similar results were obtained from amphibian rods (31). The effect of signal shortening depends on the time period of channel closure that has prevailed when the test flash is applied. The shortening is maximal when the test flash is applied during the reopening of the channels and gradually disappears by further increasing the flash separation. This preflash-induced signal shortening does not agree with the concept of an intermediate  $X^*$  being light-activated with a constant gain (Appendix 1, ii).

We observed that after a preflash, the process of signal shortening is still active after the photoreceptor current has fully recovered (Fig. 3, A and B). This finding suggests that the shortening of  $t'_c$  is not due to the cGMP concentration or the conductance state of the light-dependent channels. However, determination of the preflash-induced reduction of  $\text{Ca}_i$  showed that the shortening of  $t'_c$  and  $\text{Ca}_i$  present in the moment of the test-flash are strictly related (Fig. 3). In particular, preventing a decrease of  $\text{Ca}_i$  completely abolishes the shortening of  $t'_c$ . We therefore conclude that a preflash-induced shortening of  $t'_c$  is mainly based on the reduction of  $\text{Ca}_i$ . Hence, the dependence of  $t'_c$  shortening on the flash separation reflects the time course of  $\text{Ca}_i$  after the preflash.

In principle, the photosignal shortening may be due to either a reduced  $X^*$  lifetime  $\tau_X$  (24) or a reduced phototransduction gain (21–23,27). A reduced lifetime  $\tau_X$  was concluded from experiments with isolated enzyme preparations showing an accelerated PDE inhibition after a reduction of  $\text{Ca}_i$  (24). In contrast, in intact rods of the tiger salamander, background light shortens  $t_c$  without affecting  $\tau_X$  (22,27). We found that  $\tau_X$  was not affected by a preflash (Fig. 6 B). A similar result was reported for isolated amphibian rods (31). In

truncated rods, a reduction of  $\text{Ca}_i$  was shown to reduce the amplification of the transduction cascade (21). All of these findings give evidence for a reduced transduction gain instead of a reduced  $X^*$  lifetime  $\tau_X$ .

### Model for describing signal shortening in double flash experiments

The concept of an exponentially decaying intermediate  $X^*$  that dominates the recovery of phototransduction (Appendix 1) supposes a constant transduction gain. It describes the dependence between signal length and flash intensity only if single flashes are applied. According to our results of signal shortening in double-flash experiments, a variable transduction gain has to be introduced (Appendix 3), which is reduced by a depletion of  $\text{Ca}_i$  after a preflash.

After a flash, the reduction and reincrease of  $\text{Ca}_i$  is a dynamic process continuously changing the activity of  $\text{Ca}_i$ -regulated enzymes. It is unlikely that enzymatic activity controlling the transduction gain downstream of  $X^*$  changes in parallel to  $\text{Ca}_i$  because a gain reduction in this part of the transduction chain would lead to a nonlinear  $t_c$  relation versus  $\log(I_f/I_0)$ . In fact, linearity was observed to be independent of whether the test flash was applied to the dark-adapted retina or after a preflash (Fig. 6 B). Therefore, we suggest that  $\text{Ca}_i$  acts only on this part of the transduction chain that determines the number of  $X^*$  initially activated by the test flash, i.e., the overall gain  $\gamma$  upstream of  $X^*$  (see Appendix 1, Eq. A1a). Furthermore, to establish linearity of the  $t_c$  relation versus  $\log(I_f/I_0)$ ,  $\gamma$  must be fixed at the beginning of a photoresponse. Therefore, in accordance with others (23,28), our data suggest that generation of  $X^*$  with gain  $\gamma$  is completed in a short time period after the flash. Hence, the value of  $\gamma$  depends on  $\text{Ca}_i$  present in this time window. Then, in the dark-adapted rod, the test flash produces an initial amount  $X_0^*$  of the intermediate  $X^*$  with a gain  $\gamma_d$ . After a preflash,  $\text{Ca}_i$  is reduced and the test flash produces a lower number of  $X_0^{*'} due to a reduced gain  $\gamma_f$ . Consequently, constant background illumination should reduce  $\gamma$  to a constant value  $\gamma_b$  due to a reduced steady-state concentration of  $\text{Ca}_i$ . Regulation of  $\gamma$  is roughly estimated to be completed in a time window of  $<800$  ms after a flash by considering that just saturated photosignals start to recover 700–800 ms after the flash, with a time constant  $\tau_{\text{rec}}$  similar to  $\tau_X$ .$

By use of Eq. A7 (Appendix 3),  $\gamma_f/\gamma_d$  was calculated from the data shown in Fig. 6 A and plotted as a function of  $\Delta t_f$  (Fig. 6 C). As a result,  $\gamma_f/\gamma_d$  is reduced with a time constant of 1.1 s. The preflash can reduce  $\gamma_f$  maximally to 20% of its dark value. During the plateau phase of the preflash-induced photosignal  $\gamma_f$  is reduced independent of the flash intensity. This is in agreement with the idea that  $\text{Ca}_i$  regulates  $\gamma_f$ . Based on our result that after a preflash  $\text{Ca}_i$  is reduced with a time constant  $\tau_{\text{Ca}} = 2.3$  s at  $23^\circ\text{C}$  (8), we obtained a relation between  $\text{Ca}_i$  and  $\gamma_f/\gamma_d$  as shown in Fig. 7. Within the range in which  $\text{Ca}_i$  can be regulated by light the gain  $\gamma_f$  increases in a



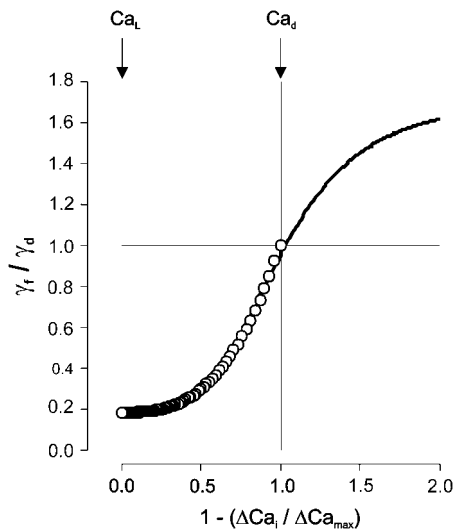


FIGURE 7 Transduction gain  $\gamma_f$  normalized to the dark value  $\gamma_d$  in dependence of the relative change of the  $\text{Ca}^{2+}$  concentration  $1 - \Delta\text{Ca}_i / \Delta\text{Ca}_{\text{max}}$ , where  $\Delta\text{Ca}_{\text{max}}$  is the maximum reduction of  $\text{Ca}_i$  achieved by intense illumination of an ROS. The data points were obtained by assuming that  $\gamma_f$  is reduced, with a time constant of 1.1 s after the preflash, whereas  $\text{Ca}_i$  is exponentially reduced from the dark level  $\text{Ca}_d$  to a minimum concentration  $\text{Ca}_L$  by a time constant  $\tau_{\text{Ca}} = 2.3$  s. Data points were fitted to a Michaelis-Menten equation assuming that  $K_m = \text{Ca}_d$ . The fit yielded a Hill coefficient  $n = 3.87$ .

sigmoidal shape from a basic light-adapted level at minimum  $\text{Ca}_i$  (at  $\text{Ca}_L$ ) to the dark-adapted value  $\gamma_d$  (at  $\text{Ca}_d$ ). Unfortunately this dose-response curve is incomplete, because data are available only for  $\text{Ca}_i$  values  $< \text{Ca}_d$ . However, the curve suggests that  $\gamma_f$  is about half maximally at  $\text{Ca}_i = \text{Ca}_d$ . Given  $K_m = \text{Ca}_d$ , we obtained a Hill coefficient  $n = 3.87$ . According to these results,  $\gamma_f$  is most sensitive to changes of  $\text{Ca}_i$  at conditions of dark adaptation. Fig. 7 suggests that a half-maximal reduction of  $\text{Ca}_i$ , which is achieved approximately by 50% reduction of the dark current, is sufficient to produce a 90% reduction of  $\gamma_f$ . Thus, the control of  $\gamma_f$  should be most distinct at light intensities below saturation of the photoresponse, i.e., at physiological levels of illumination.

### Mechanism for $\text{Ca}_i$ -dependent gain control

The enzyme representing  $X^*$  and the mechanism underlying the gain control are hitherto unknown. Originally, Pepperberg (27) suggested that  $X^*$  is catalytically active rhodopsin,  $\text{Rho}^*$ , which deactivates with a  $\tau_X$  of 1–2 s. A similar  $\text{Rho}^*$  lifetime was reported for dialyzed ROS (48). Measurements of light scattering, which was attributed to the rhodopsin-transducin interaction, yielded a  $\text{Rho}^*$  lifetime of 3–5 s (27). Actually, a  $\text{Ca}_i$  regulation of the gain  $\alpha$  (see Appendix 1), which controls the number of  $\text{Rho}^*$  generated by a flash (21), has never been measured directly. Moreover, much shorter  $\text{Rho}^*$  lifetimes of  $\sim 0.4$ – $0.5$  s were found in truncated rods at 1 mM  $\text{Ca}^{2+}$  (29) and in dark-adapted rods (at  $\text{Ca}_d$ ) of tiger

salamander. In the latter report, the lifetime of  $\text{Rho}^*$  was assumed to be further reduced by exposure to light (23). According to these reports,  $\text{Rho}^*$  deactivation is a  $\text{Ca}^{2+}$ -sensitive step that controls the amplitude of the photosignal without being rate-limiting.

Recent results suggest that  $X^*$  is  $\text{T}_\alpha\text{GTP}$  (29,30) and the rate-limiting step that terminates PDE activation is hydrolysis of GTP bound to  $\text{T}_\alpha$ . The  $\text{GTP}_{\text{ase}}$  activity of  $\text{T}_\alpha$  depends on GTPase accelerating proteins as RGS9 (30,49) and  $\text{PDE}_\gamma$  (50). In intact photoreceptors, the lifetime of  $\text{T}_\alpha\text{GTP}$  may range from 0.6 (51) up to several seconds (52), which is in the same order of magnitude as the measured values for  $\tau_X$ .

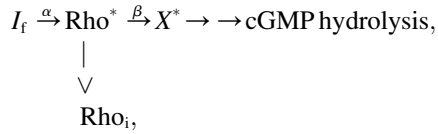
In principle, a decreased  $\text{Ca}_i$  may reduce the gain  $\gamma$  of  $\text{T}_\alpha\text{GTP}$  formation by 1), reducing the number of  $\text{Rho}^*$  activated per photon (21); 2), reducing  $\text{Rho}^*$  lifetime (23,28,53); 3), reducing the rate of  $\text{Rho}^*$ -mediated transducin activation; and 4), reducing the effective transducin level in the discs. No indication is given that  $\text{Ca}_i$  affects the gain  $\alpha$  of  $\text{Rho}^*$  formation (case 1). However, significant experimental evidence is given for a  $\text{Ca}_i$  regulation of the gain  $\beta$ , which determines the fraction of  $\text{T}_\alpha\text{GTP}/\text{Rho}^*$  (cases 2–4). The enzyme recoverin may play a major role in this respect. After  $\text{Ca}^{2+}$  unbinding, recoverin accelerates the phosphorylation of  $\text{Rho}^*$  through rhodopsin kinase (24). This may reduce the effectiveness of the  $\text{Rho}^*$ -transducin interaction and shorten the time of  $\text{T}_\alpha\text{GTP}$  formation (cases 2 and 3). Indeed, by dialysis of recoverin into an ROS (54,55) and in knockout mice  $\text{Ca}$ , recoverin increases the duration of light-induced PDE activity (56). Our estimation yields that the transduction gain has a  $K_{1/2} \geq \text{Ca}_d$  (Fig. 7), which is in good agreement with the  $K_{1/2}$  value of recoverin. Whereas  $K_{1/2}$  of recoverin in truncated rods perfused with the recombinant enzyme is in the  $\text{Ca}_i$  range of several micromolar, it is estimated to be lower, close to  $\text{Ca}_d$  in the intact cell (55). An additional mechanism (57) in accordance with the observed signal shortening is a reduction of the effective transducin level in the discs (case 4). It is known that after unphosphorylation the enzyme phosducin binds effectively to  $\text{T}_{\beta\gamma}$  which has been shown to block the interaction of transducin and  $\text{Rho}^*$  and to facilitate the translocation of transducin from the outer segments (58). Phosphorylation of phosducin is established by  $\text{Ca}/\text{calmodulin}$ -dependent protein kinase II (59).

## APPENDIX 1

### Model 1, for single-flash measurements

During the plateau phase of a saturated photosignal, all cGMP-dependent membrane channels are closed. The channels reopen during the subsequent recovery phase. According to Pepperberg et al. (27), the plateau length  $t_c$  can be derived as a function of flash intensity if the following assumptions are met:

1. The number of excited rhodopsin  $\text{Rho}^*$  per rod is proportional to the intensity of the test flash  $I_f$ :  $R_0 = \alpha \times I_f$ . An initial amount  $X_0$  of an intermediate  $X^*$  of the transduction cascade is activated proportional to  $R_0$ :  $X_0 = \beta \times R_0$ , where  $\beta$  is the system gain. This connection is demonstrated by the following simplified scheme



where  $\text{Rho}_i$  is deactivated  $\text{Rho}^*$ . Thus, the overall gain of  $X^*$  formation is  $\gamma = \alpha \times \beta$  and

$$X_0 = \gamma \times I_f. \quad (\text{A1a})$$

The deactivation of  $X^*$ , proceeding by first-order kinetics with a time constant  $\tau_X$  is the rate-limiting step in the deactivation of the transduction cascade.

$$X^* = X_0 \times e^{-t/\tau_X}. \quad (\text{A1b})$$

2. The guanylyl cyclase is maximally activated at the end of the plateau phase of a saturated photostimulus. Hence, its effect on the duration of the signal length is the same for all saturating-flash intensities.
3. When the cGMP-dependent channels start to reopen, cGMP production is balanced by a distinct rate of cGMP hydrolysis. The rate of hydrolysis at the end of the plateau phase is determined by the remainder of  $X^*$  activity,  $X_c^*$ .

In practice, we determined the signal length  $t_c$  as the time between the flash and the return of the membrane current to a certain criterion level, i.e. a fixed fraction of its dark value. This level was recognized by a recovery of the photostimulus to 50% of its maximum amplitude (cf. Fig. 2 B).  $X_c^*$  is the amount of  $X^*$  still active at this criterion level. It is

$$X_c^* = X_0 \times e^{-t_c/\tau_X}. \quad (\text{A2})$$

Since  $\tau_X$  and  $X_c^*$  are supposed to be constant, the signal length  $t_c$  is a function of  $X_0$  only:

$$t_c = \tau_X \times \ln(X_0/X_c^*).$$

According to Eq. A1a, a simple but fundamental relation follows as

$$t_c = \tau_X \times \ln(I_f/I_c), \quad (\text{A3})$$

where  $I_c$  is the flash intensity producing an amount of  $X_c^*$  of the intermediate  $X^*$ .

## APPENDIX 2

### Model 2, for double-flash recordings

A first conditioning preflash and a second test-flash are assumed to activate an amount of  $X_{0,\text{pre}} = \gamma \times I_{\text{pre}}$  and  $X_0' = \gamma \times I_f$  of the intermediate  $X^*$ , respectively. Then, if the preflash and the test-flash are separated with a time  $\Delta t_f$ , and if  $t_c'$  is the signal length of the second photostimulus, according to Eq. A2,  $X_c^*$  is given by

$$X_c^* = (X_{0,\text{pre}} \times e^{-\Delta t_f/\tau_X} + X_0') \times e^{-t_c'/\tau_X}. \quad (\text{A4})$$

Here,  $X_{0,\text{pre}} \times e^{-\Delta t_f/\tau_X}$  is the residual part of  $X^*$  remaining from the activation by the preflash at the time the second flash is fired. On the other hand, the signal length  $t_c$  of the photostimulus of the same test flash applied to a dark-adapted retina is provided by Eq. A2. Supposing that always the same amount  $X_c^*$  of intermediate is active when the photostimulus surpasses the criterion level, it is possible to relate  $t_c'$  (flash-adapted) and  $t_c$  (dark-adapted) by combining Eqs. A2 and A4:

$$(X_{0,\text{pre}} \times e^{-\Delta t_f/\tau_X} + X_0') \cdot e^{-t_c'/\tau_X} = X_0 \times e^{-t_c/\tau_X}.$$

Transformation gives the ratio of the signal lengths

$$t_c'/t_c = 1 + (\tau_X/t_c) \times \ln(X_{0,\text{pre}}/X_0 \times e^{-\Delta t_f/\tau_X} + (X_0'/X_0)). \quad (\text{A5})$$

With  $\Delta t_c = t_c' - t_c$ , it follows that

$$\Delta t_c = \tau_X \cdot \ln(X_{0,\text{pre}}/X_0 \times e^{-\Delta t_f/\tau_X} + (X_0'/X_0)). \quad (\text{A5a})$$

From Eq. A5, it can be concluded that upon variation of  $\Delta t_f$ ,  $t_c'/t_c$  should always be  $>1$ , i.e., the signal length should be prolonged as a result of a preflash.

## APPENDIX 3

### Model 3, for double flashes with variation of the system gain

Our data, as well as those of others (21,22,27,31), suggest that light adaptation causes a reduced transduction gain. We suppose a reduction of the overall gain  $\gamma$  of  $X^*$  formation, whereas the deactivation time  $\tau_X$  of the intermediate remains unchanged. Hence, if a test flash after a preflash produces an initial amount of intermediate  $X_0' = \gamma_f \times I_f$ , and if  $\gamma_f$  and  $\gamma_d$  are the overall gains in a flash- and in a dark-adapted rod, respectively, then, applying Eq. A1a, it follows that

$$X_0'/X_0 = \gamma_f/\gamma_d. \quad (\text{A6})$$

As a result, Eq. A5a can be converted to describe the change  $\Delta t_c$  of the signal length in dependence of the reduced gain  $\gamma_f$ :

$$\Delta t_c = \tau_X \times \ln(X_{0,\text{pre}}/X_0 \times e^{-\Delta t_f/\tau_X} + (\gamma_f/\gamma_d)). \quad (\text{A5b})$$

Finally, it follows that

$$\gamma_f/\gamma_d = (e^{+\Delta t_c/\tau_X} - X_{0,\text{pre}}/X_0 \cdot e^{-\Delta t_f/\tau_X}). \quad (\text{A7})$$

Assuming that the initial amount of the flash-induced intermediate is smaller after a preflash than without a preflash ( $X_0' < X_0$ ), it follows from Eq. A5b, with  $\gamma_f/\gamma_d < 1$  and  $\Delta t_f \rightarrow \infty$ , that  $\Delta t_c$  can be negative and correspondingly  $t_c'/t_c < 1$ .

This work was supported by the Deutsche Forschungsgemeinschaft projects RU 209,9-6 and 13-1.

## REFERENCES

1. Pugh, E. N., Jr., and T. D. Lamb. 1993. Amplification and kinetics of the activation steps in phototransduction. *Biochim. Biophys. Acta.* 1141: 111–149.
2. Fain, G. L., H. R. Matthews, M. C. Cornwall, and Y. Koutalos. 2001. Adaptation in vertebrate photoreceptors. *Physiol. Rev.* 81:117–151.
3. Burns, M. E., and D. A. Baylor. 2001. Activation, deactivation, and adaptation in vertebrate photoreceptor cells. *Annu. Rev. Neurosci.* 24: 779–805.
4. Yau, K. W., and K. Nakatani. 1984. Cation selectivity of light-sensitive conductance in retinal rods. *Nature.* 309:352–354.
5. Hodgkin, A. L., P. A. McNaughton, and B. J. Nunn. 1985. The ionic selectivity and calcium dependence of the light-sensitive pathway in rod rods. *J. Physiol.* 358:447–468.
6. Nakatani, K., and K. W. Yau. 1988. Calcium and magnesium fluxes across the plasma membrane of the toad rod outer segment. *J. Physiol.* 395:695–729.
7. McNaughton, P. A., L. Cervetto, and B. J. Nunn. 1986. Measurement of the intracellular free calcium concentration in salamander rods. *Nature.* 322:261–263.

8. Knopp, A., and H. R  ppel. 1996.  $\text{Ca}^{2+}$  fluxes and channel regulation in rods of the albino rat. *J. Gen. Physiol.* 107:577–595.
9. Yoshikami, S., J. S. George, and W. A. Hagins. 1980. Light-induced calcium fluxes from outer segment layer of vertebrate retinas. *Nature*. 286:395–398.
10. Gold, G. H. 1986. Plasma membrane calcium fluxes in intact rods are inconsistent with the “calcium hypothesis”. *Proc. Natl. Acad. Sci. USA*. 83:1150–1154.
11. Ratto, G., R. Payne, W. G. Owen, and R. Y. Tsien. 1988. The concentration of cytosolic free calcium in vertebrate rod outer segments measured with fura-2. *J. Neurosci.* 8:3240–3246.
12. Yau, K. W., and K. Nakatani. 1985. Light-induced reduction of cytoplasmic free calcium in retinal rod outer segment. *Nature*. 313: 579–582.
13. McCarthy, S. T., J. P. Younger, and W. G. Owen. 1994. Free calcium concentrations in bullfrog rods determined in the presence of multiple forms of fura-2. *Biophys. J.* 67:2076–2089.
14. Mc Carthy, S. T., J. P. Younger, and W. G. Owen. 1996. Dynamic, spatially nonuniform calcium regulation in frog rods exposed to light. *J. Neurophysiol.* 76:1991–2004.
15. Nakatani, K., and K. W. Yau. 1988. Calcium and light adaptation in retinal rods and cones. *Nature*. 334:69–71.
16. Matthews, H. R. 1991. Incorporation of chelator into guinea-pig rods shows that calcium mediates mammalian light adaptation. *J. Physiol.* 436:93–105.
17. Matthews, H. R. 1995. Effects of lowered cytoplasmic calcium concentration and light on the responses of salamander rod photoreceptors. *J. Physiol.* 484:267–286.
18. Koch, K.-W., and L. Stryer. 1988. Highly cooperative feedback control of retinal rod guanylate cyclase by calcium ions. *Nature*. 334:64–66.
19. Koutalos, Y., K. Nakatani, and K. W. Yau. 1995. The cGMP-phosphodiesterase and its contribution to sensitivity regulation in retinal rods. *J. Gen. Physiol.* 106:891–921.
20. Nikonov, S., N. Engheta, and E. N. Pugh, Jr. 1998. Kinetics of recovery of the dark-adapted salamander rod photoresponse. *J. Gen. Physiol.* 111:7–37.
21. Lagnado, L., and D. A. Baylor. 1994. Calcium controls light-triggered formation of catalytically active rhodopsin. *Nature*. 367:273–277.
22. Pepperberg, D. R., J. Jin, and G. J. Jones. 1994. Modulation of transduction gain in light adaptation of retinal rods. *Vis. Neurosci.* 11:53–62.
23. Matthews, H. R. 1997. Actions of  $\text{Ca}^{2+}$  on an early stage in phototransduction revealed by the dynamic fall in  $\text{Ca}^{2+}$  concentration during the bright flash response. *J. Gen. Physiol.* 109:141–146.
24. Kawamura, S. 1993. Rhodopsin phosphorylation as a mechanism of cyclic GMP phosphodiesterase regulation by S-modulin. *Nature*. 362: 855–857.
25. Hsu, Y. T., and R. S. Molday. 1993. Modulation of the cGMP-gated channel of rod photoreceptor cells by calmodulin. *Nature*. 361:76–79. Erratum in *Nature*. 365:279.
26. Baylor, D. A., A. L. Hodgkin, and T. D. Lamb. 1974. Reconstruction of the electrical responses of turtle cones to flashes and steps of light. *J. Physiol.* 242:759–791.
27. Pepperberg, D. R., M. C. Cornwall, M. Kahlert, K. P. Hofmann, J. Jin, G. J. Jones, and H. Ripps. 1992. Light-dependent delay in the falling phase of retinal rod photoresponse. *Vis. Neurosci.* 8:9–18.
28. Lyubarsky, A., S. Nikonov, and E. N. Pugh, Jr. 1996. The kinetics of inactivation of the rod phototransduction cascade with constant  $\text{Ca}^{2+}_i$ . *J. Gen. Physiol.* 107:19–34.
29. Sagoo, M. S., and L. Lagnado. 1997. G-protein deactivation is rate-limiting for shut-off of the phototransduction cascade. *Nature*. 389: 392–395.
30. Chen, C. K., M. E. Burns, W. He, T. G. Wensel, D. A. Baylor, and M. I. Simon. 2000. Slowed recovery of rod photoresponse in mice lacking the GTPase accelerating protein RGS9-1. *Nature*. 403:557–560.
31. Murnick, J. G., and T. D. Lamb. 1996. Kinetics of desensitization induced by saturating flashes in toad and salamander rods. *J. Physiol.* 495:1–13.
32. Hagins, W. A., R. D. Penn, and S. Yoshikami. 1970. Dark current and photocurrent in retinal rods. *Biophys. J.* 10:380–412.
33. Penn, R. D., and W. A. Hagins. 1972. Kinetics of the photocurrent of retinal rods. *Biophys. J.* 12:1073–1094.
34. Knopp, A. 1994. Kalziumfl  sse, Kanalregulierung und Rhodopsin-deaktivierung im Vertebraten-Sehst  bchen. Verlag Shaker, Aachen, Germany.
35. Miller, D. L., and J. I. Korenbrot. 1987. Kinetics of light-dependent  $\text{Ca}$  fluxes across the plasma membrane of rod outer segments. *J. Gen. Physiol.* 90:397–425.
36. Yau, K. W., and K. Nakatani. 1984. Electrogenic Na-Ca exchange in retinal rod outer segment. *Nature*. 311:661–663.
37. Cervetto, L., L. Lagnado, R. J. Perry, D. W. Robinson, and P. A. McNaughton. 1989. Extrusion of calcium from rod outer segments is driven by both sodium and potassium gradients. *Nature*. 337:740–743.
38. Lagnado, L., L. Cervetto, and P. A. McNaughton. 1988. Ion transport by the Na-Ca exchange in isolated rod outer segments. *Proc. Natl. Acad. Sci. USA*. 85:4548–4552.
39. Friedel, U., G. Wolbring, P. Wohlfart, and N. J. Cook. 1991. The sodium-calcium exchanger of bovine rod photoreceptors:  $\text{K}^{+}$ -dependence of the purified and reconstituted protein. *Biochim. Biophys. Acta*. 1061:247–252.
40. Fain, G. L., and J. E. Lisman. 1981. Membrane conductances of photoreceptors. *Prog. Biophys. Mol. Biol.* 37:91–147.
41. Robinson, D. W., G. M. Ratto, L. Lagnado, and P. A. McNaughton. 1993. Temperature dependence of the light response in rat rods. *J. Physiol.* 462:465–481.
42. Baylor, D. A., G. Matthews, and K. W. Yau. 1983. Temperature effects on the membrane current of retinal rods of the toad. *J. Physiol.* 337: 723–734.
43. Lamb, T. D. 1984. Effects of temperature changes on toad rod photocurrents. *J. Physiol.* 346:557–578.
44. Forti, S., A. Menini, and G. Rispoli. 1989. Kinetics of phototransduction in retinal rods of the newt *Triturus cristatus*. *J. Physiol.* 419:265–295.
45. Lyubarsky, A. L., and E. N. Pugh, Jr. 1996. Recovery phase of the murine rod photoresponse reconstructed from electroretinographic recordings. *J. Neurosci.* 16:563–571.
46. Lagnado, L., L. Cervetto, and P. A. McNaughton. 1992. Calcium homeostasis in the outer segments of retinal rods from the tiger salamander. *J. Physiol.* 455:111–142.
47. Dizhoor, A. M., and J. B. Hurley. 1999. Regulation of photoreceptor membrane guanylyl cyclases by guanylyl cyclase activator proteins. *Methods*. 19:521–531.
48. Rieke, F., and D. A. Baylor. 1998. Origin of reproducibility in the response of retinal rods to single photons. *Biophys. J.* 75:1836–1857.
49. He, W., C. W. Cowan, and T. G. Wensel. 1998. RGS9, a GTPase accelerator for phototransduction. *Neuron*. 20:95–102.
50. Tsang, S. H., M. E. Burns, P. D. Calvert, P. Gouras, D. A. Baylor, S. P. Goff, and V. Y. Arshavsky. 1998. Role for the target enzyme in deactivation of photoreceptor G protein in vivo. *Science*. 282:117–121.
51. Vuong, T. M., and M. Chabre. 1991. Deactivation kinetics of the transduction of vision. *Proc. Natl. Acad. Sci. USA*. 88:9813–9817.
52. Arshavsky, V. Y., M. P. Antoch, and P. P. Philippov. 1987. On the role of transducin GTPase in the quenching of a phosphodiesterase cascade of vision. *FEBS Lett.* 224:19–22.
53. Wagner, R., N. Ryba, and R. Uhl. 1989. Calcium regulates the rate of rhodopsin disactivation and the primary amplification step in visual transduction. *FEBS Lett.* 242:249–254.
54. Gray-Keller, M. P., A. S. Polans, K. Palczewski, and P. B. Detwiler. 1993. The effect of recoverin-like calcium-binding proteins on the photoresponse of retinal rods. *Neuron*. 10:523–531.

55. Erickson, M. A., L. Lagnado, S. Zozulya, T. A. Neubert, L. Stryer, and D. A. Baylor. 1998. The effect of recombinant recoverin on the photoresponse of truncated rod photoreceptors. *Proc. Natl. Acad. Sci. USA.* 95:6474–6479.
56. Makino, C. L., R. L. Dodd, J. Chen, M. E. Burns, A. Roca, M. I. Simon, and D. A. Baylor. 2004. Recoverin regulates light-dependent phosphodiesterase activity in retinal rods. *J. Gen. Physiol.* 123:729–741.
57. Heck, M., and K. P. Hofmann. 2001. Maximal rate and nucleotide dependence of rhodopsin-catalyzed transducin activation: initial rate analysis based on a double displacement mechanism. *J. Biol. Chem.* 276:10000–10009.
58. Sokolov, M., K. J. Strissel, I. B. Leskov, N. A. Michaud, V. I. Govardovskii, and V. Y. Arshavsky. 2004. Phosducin facilitates light-driven transducin translocation in rod photoreceptors. Evidence from the phosducin knockout mouse. *J. Biol. Chem.* 279:19149–19156.
59. Thulin, C. D., J. R. Savage, J. N. McLaughlin, S. M. Truscott, W. M. Old, N. G. Ahn, K. A. Resing, H. E. Hamm, M. W. Bitensky, and B. M. Willardson. 2001. Modulation of the G protein regulator phosducin by Ca<sup>2+</sup>/calmodulin-dependent protein kinase II phosphorylation and 14–3–3 protein binding. *J. Biol. Chem.* 276:23805–23815.